Title: IGF2 induces CD133 expression in esophageal cancer cells to promote cancer stemness

Running title: IGF2 induces CD133 to promote cancer stemness

Wen Wen Xu[1,2,], Bin Li[1,3,*], Jian Fu Zhao[4], Jing Ge Yang[5], Jun Qi Li[2], Sai Wah Tsao[1], Qing-Yu He[3], Annie LM Cheung[1*]

[1]School of Biomedical Sciences, Li Ka Shing Faculty of Medicine, The University of Hong Kong, Pokfulam, Hong Kong SAR, China; [2]Institute of Biomedicine, Guangdong Provincial Key Laboratory of Bioengineering Medicine, National Engineering Research Center of Genetic Medicine, Jinan University, Guangzhou, China; [3]Key Laboratory of Functional Protein Research of Guangdong Higher Education Institutes, Institute of Life and Health Engineering, College of Life Science and Technology, Jinan University, Guangzhou 510632, China; [4]Department of Oncology, First Affiliated Hospital, Jinan University, Guangzhou 510632, China, [5]Department of General Surgery, First Affiliated Hospital, Jinan University, Guangzhou 510632, China.

Correspondence Author:

Dr. Annie L. M. Cheung, School of Biomedical Sciences, Li Ka Shing Faculty of Medicine, The University of Hong Kong, 21 Sassoon Road, Pokfulam, Hong Kong SAR, China. Phone: (852) 39179293; Fax: (852) 28170857; Email: lmcheung@hku.hk.

Dr. Bin Li, Key Laboratory of Functional Protein Research of Guangdong Higher Education Institutes, Institute of Life and Health Engineering, College of Life Science and Technology,

Jinan University, Guangzhou, China. Phone: (86)-20-85224372; Fax: (86)-20-85224372; Email: libin2015@jnu.edu.cn.

Conflict of interest statement: The authors declare no conflict of interest.

Abstract

Failure to eradicate cancer stem cells (CSC) during primary therapy may lead to cancer recurrence. We recently reported that CD133 is a functional biomarker for CSCs in esophageal squamous cell carcinoma (ESCC) but the molecular pathways critical for maintenance of CD133-positive CSCs are largely unknown. Here, we revealed that knockdown of IGF2 or treatment with PI3K/AKT inhibitors markedly inhibited the abilities of CD133-positive ESCC cells to self-renew, resist chemotherapeutic drugs, and form tumors. Further functional analysis identified miR-377 as a downstream regulator of PI3K/AKT signaling, and a mediator of the effects of IGF2 on CD133 expression and CSC properties. We found that the expression levels of IGF2 and CD133 were positively correlated with each other in primary ESCC, and that concurrent elevation of IGF2 and CD133 expression was significantly associated with poor patient survival. Furthermore, *in vivo* experiments demonstrated that IGF2-neutralizing antibody enhanced the sensitivity of tumor xenografts in nude mice to 5-fluorouracil treatment. This study underpins the importance of the IGF2-PI3K/AKT-miR-377-CD133 signaling axis in the maintenance of cancer stemness and in the development of novel therapeutic strategy for treatment of esophageal cancer.

Keywords: cancer stem cells, esophageal cancer, CD133, prognostic biomarker, targeted therapy

1. Introduction

Esophageal cancer is the one of the deadliest and least studied cancers worldwide. The prognosis is very poor and the 5-year survival rate is less than 20% [1]. However, the precise mechanisms and genetic underpinnings of this disease remain to be fully elucidated. Therefore, there is an urgent need to test novel biomarkers for diagnostic and prognostic significances, and to explore their potentials as therapeutic targets.

The existence of cancer cells with stem-like properties that have the capacity to resist conventional chemoradiotherapy and to self-renew is one of the major challenges in cancer treatment. Previous studies have established a link between chemoresistance and cancer stem cells (CSCs) phenotype [2, 3]. CD133 is a five transmembrane domain cell surface glycoprotein originally found on neuroepithelial stem cells in mice [4]. CD133 has been used as a marker to isolate CSCs from diverse solid tumors such as hepatocellular carcinoma [5] and colon cancer [6]. CD133 has also been reported to be associated with worse overall survival and higher recurrence rates in several cancer types [5, 7, 8]. There are very few reports regarding the significance of CD133 in the context of esophageal cancer. In our recent study, we provided the first evidence that CD133 is a functional CSC marker for esophageal squamous cell carcinoma (ESCC) [9]. However, we are still far from fully understanding the molecular mechanisms that drive CSC maintenance in ESCC.

Insulin-like growth factors (IGF) play important roles in many tumor proliferation, growth, differentiation, and angiogenesis, and are therefore regarded as promising targets in cancer therapy [10, 11]. Although insulin-like growth factors 1 (IGF1) and insulin-like growth factor 2 (IGF2) share about 70% homology in amino acid sequence, they each have their distinct functions. In our previous studies, we showed that overexpression of Inhibitor of Differentiation 1 (Id1) induces the expression of IGF2, which can promote cancer

progression in both autocrine and paracrine manners [12, 13]. However, the functional role and mechanism of IGF2 in tumor initiation and cancer stemness remain to be elucidated. In the present study, we determined if IGF2 is functionally required for the maintenance of CSC properties in ESCC cells by performing *in vitro* and *in vivo* experiments to study its effects on the stem cell marker CD133 and CSC phenotypes including chemoresistance, tumor initiation and self-renewal. Whether blockade of IGF2 signal with neutralizing antibody could suppress the ability of ESCC cells to form spheres *in vitro* and tumors *in vivo* was also examined.

2. Materials and Methods

2.1 Cell culture and drugs

Human ESCC cell lines KYSE270 (DSMZ, Braunschweig, Germany) [14] and T.Tn [15] were maintained in RPMI 1640 (Sigma, St. Louis, MO, USA) supplemented with 10% fetal bovine serum (Invitrogen, Gaithersburg, MD, USA) at 37ºC in 5% CO_2. Human recombinant IGF2 was purchased from Invitrogen. Wortmannin, LY294002, 5-fluorouracil (5-FU) and cisplatin, purchased from Calbiochem (Darmstadt, Germany), were dissolved in dimethyl sulfoxide (DMSO).

2.2 Transfection, transduction, and establishment of stable cell lines

The miR-377 mimic and negative control, and the anti-miR-377 inhibitor and corresponding negative control, were purchased from Thermo Scientific Ambion (Austin, TX, USA). The plasmid expressing phosphatase and tensin homolog (PTEN), i.e. pcDNA3-PTEN [16], and the vector control pcDNA3-GFP [17] were gifts from William Sellers (Dana Faber Cancer Institute, Boston, MA, USA) and Alonzo Ross (University of Massachusetts, Worcester, MA, USA), respectively (Addgene plasmids 10759 and 20738; Addgene, Cambridge, MA, USA). Transfection and establishment of stable cell lines with knockdown of IGF2 were performed as described previously [18], and stable cell lines were obtained after further selection with puromycin.

2.3 Isolation of $CD133^+$ and $CD133^-$ populations by flow cytometry

Cell sorting was performed as described previously [9]. In brief, cells were stained with phycoerythrin (PE)-conjugated anti-human CD133 antibody (Miltenyi Biotec, Bergisch Gladbach, Germany) or with isotype control mouse IgG1-PE (Miltenyi Biotec), and then analyzed and sorted on BD FACS Aria I (BD Biosciences, San Jose, CA). The top 20% of most brightly stained cells and the bottom 20% of most dimly stained cells were selected as positive and negative populations, respectively.

2.4 Western blot

Preparation of cell and tumor lysates, and details of western blotting were described previously [19]. The primary antibodies used included phospho-AKT (Ser473), AKT and PTEN obtained from Cell Signaling Technology (Beverly, MA), IGF2 (R&D Systems, Minneapolis, MN, USA), CD133 (Miltenyi Biotec), and actin from Santa Cruz Biotechnology (Santa Cruz, CA, USA).

2.5 Quantitative real-time PCR (qRT-PCR)

Total RNA was isolated using Trizol reagent according to the manufacture's protocol (Invitrogen). Expression levels of miR-377 and U6 (internal control) were detected using Taqman microRNA reverse transcription kit and Taqman miRNA assays (Applied Biosystems, Carlsbad, CA, USA) as described previously [9]. All the experiments were performed on MyIQTM2 Real-Time PCR Detection System (Bio-Rad, Hercules, CA, USA).

2.6 MTT assay

MTT assay was carried out as described previously [20]. The absorbance was measured at a wavelength of 570 nm on a Labsystems Multiskan microplate reader (Merck Eurolab, Dietikon, Switzerland).

2.7 Sphere-formation assay

Sphere-formation assay was carried out as described previously [9]. In brief, ESCC cells were seeded onto polyHEMA (Sigma)-coated 6-well-plates, and grown in DMEM/F12 (Invitrogen) medium containing various growth factors. For serial passaging, the spheres were collected and dissociated into single cells, and then re-suspended in the above medium to culture next-generation spheres.

2.8 Tumorigenicity in nude mice

All the animal experiments were approved by the Committee on the Use of Live Animals in Teaching and Research, the University of Hong Kong, or Jinan University. Female BALB/c nude mice aged 6-8 weeks were used. Tumor xenograft experiments and determination of tumor volume were performed as described previously [21]. In the wortmannin experiment, the mice were randomized into treatment and control groups when the subcutaneous tumors reached ~5 mm diameter, and then injected intraperitoneally with wortmannin (0.6 mg/kg, every three days) and DMSO, respectively. In the IGF2 immunoneutralization experiment, groups of mice (n = 6/group) received twice weekly intratumoral injections of the neutralizing antibody against human IGF2 (Anti-IGF2, 10 $\mu g/cm^3$ tumor; R&D Systems), intraperitoneal injections of 5-FU (20 mg/kg), or anti-IGF2 combined with 5-FU, whereas the control group received DMSO or the isotype IgG. Tumors were collected at the end of

experiments. Those animals engrafted with cancer cells but with no sign of tumor burden were sacrificed and dissected 3 months after tumor cell inoculation to confirm that there was no tumor development.

2.9 Patient samples

Use of all human samples was approved by the committees for ethical review of research involving human subjects at the Queen Mary Hospital in Hong Kong and Zhengzhou University in Zhengzhou.

2.10 Tissue microarray and immunohistochemistry

A tissue microarray containing 100 cases of human ESCC (1 core/case) of which 80 had matched normal adjacent tissue (1 core/case) on the same slide (#HEso-Squ180Sur-04, Shanghai Outdo Biotech, Shanghai, China) was used to determine the correlation between IGF2 and CD133 expressions, and to evaluate the clinical significance of the two proteins in ESCC. After antigen retrieval and blocking with normal serum, the slides were incubated overnight at 4 ºC with the primary antibody against IGF2 (R&D Systems) or CD133 (Miltenyi Biotec), followed by biotinylated secondary antibodies and peroxidase-conjugated avidin-biotin complex (DAKO Diagnostics, Mississauga, ON, USA). Immunostaining was visualized using 3, 3'-diaminobenzidine (DAKO) as chromogen, and then the sections were counterstained with hematoxylin. Evaluation of IGF2 immunostaining was performed as described previously [12]. The sections were examined by two independent observers who were blinded to the patients' clinical information. Specimens assigned scores of 0 to 1 were categorized as low expression, whereas scores 2 to 3 were considered high expression. CD133 immunostaining in the TMA was evaluated in random fields under × 400

magnification. Tumors with > 1% of the tumor cells showing positive staining in the membrane and cytoplasm were defined as CD133-positive [22, 23]. Normal esophageal epithelium was scored according to the same criteria.

2.11 Analysis of TCGA data

Data sets were downloaded from LinkedOmics (http://www.linkedomics.org), which is a publicly available portal that includes multi-omics data from all 32 cancer types from The Cancer Genome Atlas (TCGA) project.

2.12 Statistical analysis

All *in vitro* experiments and assays were repeated at least three times, and the data were expressed as the mean ± SD and compared using ANOVA. The correlation between the expression levels of IGF2 and CD133, and that between IGF2 and miR-377 were assessed using Pearson rank correlation coefficient. Correlations between IGF2 or CD133 and clinicopathological parameters were determined using Fisher exact test. The association between IGF2/CD133 expressions and patient survival was plotted using the Kaplan-Meier method, and statistical differences were compared using the log-rank test. Univariate and multivariate survival analyses were performed using the Cox proportional hazard model with a forward stepwise procedure (the entry and removal probabilities were 0.05 and 0.10, respectively). *P* values < 0.05 were deemed significant.

3. Results

3.1 IGF2 is essential for tumor initiation and self-renewal in ESCC

The role of IGF2 in inducing CSC phenotype is still unclear. The significant effect of IGF2 in promoting chemoresistance in ESCC cells [18] prompted us to determine whether IGF2 is functionally crucial for maintenance of CSC properties. KYSE270 cells with IGF2-knockdown (designated KYSE270-shIGF2#2) and control cells expressing non-effective shRNA (i.e. KYSE270-shCON) were injected subcutaneously into the flanks of nude mice for comparison of tumor-initiating ability. Our results showed that even though both KYSE270-shIGF2#2 and KYSE270-shCON cell lines formed tumors in all the mice in the respective groups (n = 6) at a cell dose of $1x10^5$, the tumors in the former group were significantly smaller (**Figure 1A**). At a lower cell dose of $2x10^4$, KYSE270-shIGF2 cells formed tumors in only three out of six mice (50.0%), whereas KYSE270-shCON cells produced tumors in all six mice in the group (100%) (**Figure 1B**), indicating that IGF2 is essential for ESCC tumorigenesis. Moreover, inoculation of the same number (i.e. $2x10^4$) of resuspended cancer cells from excised primary xenografts into secondary mouse recipients produced similar results (**Figure 1B**), which suggests that IGF2 has a functional role in maintaining the sphere-forming and tumorigenic potential of ESCC cells. To further examine the significance of IGF2 in regulating CSC properties in ESCC, we determined the effects of exogenous IGF2 on the ability of KYSE270 and T.Tn cells to form spheres over serial passages in non-adherent, serum-free, growth factor-supplemented medium. As shown in **Figure 1C**, IGF2 stimulated ESCC cells to form spheres in first and second passages, but these effects were abrogated by simultaneous addition of a PI3K inhibitor, LY294002. The reduced capacity of KYSE270 and T.Tn cells with IGF2-knockdown to undergo serial propagation under sphere-formation culture conditions further confirmed that IGF2 is important for maintaining cancer stemness in ESCC (**Figure 1D**). Moreover, exposure to

IGF2 significantly increased CD133 expression in ESCC cells, and these effects were abrogated by LY294002 (**Figure 1E**). Conversely, knockdown of IGF2 significantly inhibited the expression level of CD133 (**Figure 1F**). Collectively, these results demonstrated that IGF2 is essential for maintenance of CSC properties in ESCC cells.

3.2 PI3K/AKT inhibition decreases CD133 expression and suppresses CSC phenotypes of $CD133^+$ ESCC cells

Since both CD133 [9] and phosphorylated AKT (p-AKT) expressions were increased in sphere-forming ESCC cells compared with their differentiated adherent counterparts (**Figure 2A**), we hypothesized that blockade of PI3K/AKT may suppress the CSC phenotypes of $CD133^+$ ESCC cells. We treated ESCC cells with two specific inhibitors of PI3K (i.e. wortmannin and LY294002) which were verified to produce dose-dependent inhibition of p-AKT (**Figure 2B**), and the results showed that PI3K/AKT inhibition not only reduced CD133 expression (**Figure 2B**), but also the serial sphere-formation ability of ESCC cells (**Supplementary Figure S1A**). Transfecting the cells with the vector expressing PTEN produced similar results (**Figure 2C and Supplementary Figure S1B**). We then examined whether inactivation of the PI3K/AKT pathway could preferentially target and inhibit the stemness of $CD133^+$ ESCC CSCs. Compared with sorted $CD133^-$ ESCC cells, $CD133^+$ cells were more responsive to wortmannin and LY294002 treatment (**Figure 2D**), and their ability to form spheres and to serially propagate *in vitro* was significantly suppressed by these inhibitors (**Figure 2E**). Wortmannin and LY294002 also reduced the expression level of CD133 in the sorted $CD133^+$ cells (**Figure 2F**). More importantly, growth of tumor xenografts derived from $CD133^+$ ESCC cells was significantly suppressed in nude mice treated with wortmannin (**Figure 2G**). We next studied the effects of PI3K/AKT inhibition

on the chemosensitivity of $CD133^+$ CSCs. The data from sphere-formation assays showed that PI3K/AKT inhibition rendered the $CD133^+$ ESCC cells more sensitive to 5-FU and cisplatin (DDP) treatment (**Figure 2H**). Taken together, the above findings substantiate that blockade of PI3K/AKT pathway could reduce the stemness of $CD133^+$ esophageal CSCs.

3.3 MiR-377 upregulated by PI3K/AKT inhibition mediates the effects of IGF2 on CD133 expression and CSC properties

Our recent study showed that miR-377, which can suppress the initiation of esophageal cancer by inhibiting CD133, is underexpressed in ESCC [9]. The mechanisms that downregulate miR-377 in ESCC had not been explored. Quantitative real time PCR (qRT-PCR) data indicated that PI3K/AKT inhibition increased the expression level of miR-377 in ESCC cells (**Figure 3A**). On the other hand, addition of exogenous IGF2 significantly reduced miR-377 expression in ESCC cells, and these effects were abrogated by LY294002 (**Figure 3B**). Conversely, knockdown of IGF2 expression resulted in an increase in miR-377 expression (**Figure 3C**). Moreover, KYSE270-shIGF2#2 tumor xenografts had markedly higher expression level of miR-377 and lower expression level of CD133 compared with control tumors (**Figure 3D**). These results demonstrate that IGF2 can negatively regulate miR-377 and induce CD133 expression. In another experiment, KYSE270 and T.Tn cells transfected with miR-377 mimic or negative control (miR-CON) were treated with IGF2. Western blot data showed that IGF2 induced CD133 expression in ESCC cells transfected with miR-CON, but not in cells transfected with miR-377 (**Figure 3E**). Furthermore, we found that whereas IGF2-knockdown increased 5-FU chemosensitivity and decreased sphere-forming ability of ESCC cells, transfection of miR-377 inhibitor significantly attenuated these effects (**Figure 3F and 3G**). Together, these results support that miR-377 plays a role

in mediating the effects of IGF2 on CD133 expression and CSC properties in ESCC cells. We also compared sorted $CD133^+$ and $CD133^-$ ESCC cell lines for the expression of IGF2-PI3K/AKT-miR-377-CD133 signaling axis using Western blot and Taqman miRNA assay (**Supplementary Figure S2B and 2C**). The upregulation of IGF2 and p-AKT in the $CD133^+$ cells, coupled with low miR-377 expression, strongly support the existence of a IGF2-PI3K/AKT-miR-377-CD133 cascade in maintaining CSCs (**Figure 3H**).

3.4 IGF2 is a promising therapeutic target for esophageal cancer

We recently reported elevated IGF2 level in the serum of patients with ESCC [13]. We next evaluated IGF2 as a therapeutic target for ESCC by blocking it through immunoneutralization. Tumor-sphere formation of KYSE270 and T.Tn cells was measured in the presence of IGF2-neutralizing antibody or isotype IgG control antibody. The results showed that IGF2-neutralizing antibody exerted a significant dose-dependent inhibitory effect on the sphere-forming capability of ESCC cells *in vitro* (**Figure 4A**). Tumorigenicity assay showed that treatment of tumor-bearing mice with IGF2-neutralizing antibody markedly suppressed growth of KYSE270 tumor xenografts (**Figure 4B**), as in the case of tumor xenografts established from another ESCC cell line KYSE150 [12], thus confirming that IGF2 supports tumorigenesis in ESCC. Similar to the findings in tumor xenografts derived from IGF2-knockdown ESCC cells (**Figure 3D**), treatment with IGF2-neutralizing antibody significantly increased miR-377 expression and decreased expression level of CD133 (**Figure 4C**). We also evaluated the potential of IGF2-neutralizing antibody in combinational therapy for esophageal cancer. Nude mice with established subcutaneous tumor xenografts were treated with 5-FU and IGF2-neutralizing antibody alone or in combination, and the results showed that IGF2-neutralizing antibody markedly enhanced the sensitivity of tumor xenografts to 5-

289 FU treatment (**Figure 4D**). These data suggest that immunoneutralization of IGF2 can render
290 ESCC tumors more susceptible to 5-FU treatment.

291

292 **3.5 Clinical significance of immunohistochemical expression of IGF2 and CD133 in**
293 **ESCC**

294 We reported previously that serum IGF2 level has prognostic value in ESCC [13] but whether
295 the immunohistochemical expression level of this biomarker in ESCC tissue has diagnostic
296 significance is not well documented. A tissue microarray containing 100 cases of ESCC and
297 80 cases of tumor-adjacent normal esophageal tissue was immunostained for IGF2. Examples
298 of ESCC with staining scores from 0 to 3 are shown in **Figure 5A**. As seen in **Figure 5B**, the
299 expression of IGF2 in tumors was found to be higher than that in normal adjacent tissues. We
300 then correlated IGF2 expression with clinicopathological parameters by stratifying the 100
301 patients based on the expression level of IGF2 protein. The associations between IGF2
302 protein expression and various clinicopathological parameters are presented in **Table 1**,
303 which shows a significant correlation between high IGF2 expression and tumor (T)
304 stage. Using the same tissue microarray, we further determined the expression of CD133 and
305 its correlation with clinicopathological parameters (**Figure 5C and Table 2**). In contrast to
306 normal tissue in which only 21.25% of the cases were positive for CD133, 45% of tumor
307 samples were CD133-positive (**Figure 5D**). Furthermore, concurrent elevation of IGF2 and
308 positive CD133 staining in the ESCC was associated with T3/T4 stages (**Table 3**).

309 We then determined whether immunohistochemical IGF2 and CD133 expressions were
310 associated with survival outcome. The data showed that the patients with low IGF2
311 expression in the primary tumors had better survival outcome than those with high IGF2

expression (median survival: 25.0 vs 14.0 months; log rank test, $P < 0.05$) (**Figure 5E, left panel**). Our analysis also showed that patients with CD133-negative ESCC had much longer overall survival than those with CD133-positive tumors (median survival: 25.5 vs 13.0 months; $P < 0.05$ (**Figure 5E, middle panel**). Notably, patients with concomitant high IGF2 and positive CD133 expression had a median survival time of only 9.0 months, which was significantly shorter than that of patients with low IGF2 and negative CD133 expression (median survival = 26.0 months) (**Figure 5E, right panel**). Moreover, multivariate analysis showed that concomitant high IGF2 and positive CD133 expression in tumor was an independent prognostic factor for overall survival (**Table 4**).

3.6 Correlation between IGF2 and other markers

The correlation between the expression levels of IGF2 and CD133, and that between IGF2 and miR-377 were determined in 47 pairs of ESCC and corresponding adjacent non-tumorous tissues, which were previously assayed for IGF2 and CD133 using western blotting and for miR-377 using qRT-PCR [9, 18]. The results showed that the expression levels of IGF2 and CD133 were positively correlated, whereas IGF2 and miR-377 were negatively correlated (**Figure 6A**). Further analysis based on TCGA data revealed that IGF2 and CD133 were positively correlated in several other cancer types (**Figure 6B**).

4. Discussion

IGF2 has been reported to play a very precise function in adult hematopoietic stem cell homeostasis [24]. However, there is little information about its role in cancer stem cells. The ability to initiate tumor and self-renew are well-recognized characteristics of CSCs. Here, we showed for the first time that IGF2 can drive stemness in ESCC, as evidenced by its ability to potentiate and maintain the self-renewal capacity of ESCC cells during serial passaging. The results of the present study also demonstrated that IGF2 upregulates CD133, which is a functional CSC marker in ESCC [9]. Surprisingly, relatively little is known about the upstream regulation of CD133 despite it being a widely accepted stem cell marker. Increasing evidence suggests the important roles for noncoding RNAs in cancer stem cells [25, 26]. One study showed that growth and self-renewal of CD133-positive liver CSCs are regulated by miR-230b via tumor protein 53-induced nuclear protein 1 [5]. CD133-positive liver and brain CSCs have been reported to be dependent on STAT3 signaling to promote chemoresistance and drive medulloblastoma recurrence [27, 28]. A recent study showed that CD133 confers cancer stem-like cell properties by stabilizing EGFR-AKT signaling in hepatocellular carcinoma [29]. In our present study, we found that IGF2 increased CD133 expression through downregulation of miR-377 expression in a PI3K/AKT-dependent manner **(Figures 1-3)**. Immunohistochemical analysis of a tissue microarray confirmed that the expression levels of IGF2 and CD133 were significantly correlated in ESCC tissues and more importantly, the data showed that patients with concurrent elevation of IGF2 and CD133 expressions in their primary tumors have particularly poor prognosis **(Figure 5)**. By analyzing the TCGA data, we also showed that a positive correlation between IGF2 and CD133 is common in several other cancer types **(Figure 6).**

Data from our previous studies showed that a $CD133^-$ ESCC cell line expresses IGF2 and p-AKT [9, 18, 21] which suggests that the IGF2-PI3K/AKT part of the IGF2-PI3K/AKT-

357 miR-377-CD133 axis is operative in $CD133^-$ cells although the mechanisms downstream of
358 PI3K/AKT that promote tumorigenicity in these cells may be different from that of $CD133^+$
359 cells. It should be noted that in addition to CD133, a number of promising markers of
360 esophageal CSCs have been documented, e.g. CD90, ALDH1, Lgr5, CD44; overlapping
361 expression of stem cell markers is also very common [30, 31]. $CD90^+$ esophageal cancer cells,
362 for example, have an aggressive signature and metastatic capacity [32]. It was reported that
363 the NFκB signaling pathway contributes to the acquisition of CSC-like phenotype of $CD90^+$
364 cells [33]. It is possible that $CD133^-$ cells express CD90, in which case the mechanisms
365 underlying CSC-like phenotype of $CD90^+$ cells may apply. Nevertheless, the delineation of
366 an IGF2-PI3K/AKT-miR-377-CD133 signaling pathway (**Figure 3H**) not only provides new
367 insight into the ESCC tumorigenic process, but also reveals a cascade of potential therapeutic
368 targets that may be exploited to effectively eradicate esophageal CSCs. At the top of this
369 cascade, IGF2 is increasingly recognized as an attractive therapeutic target due to its
370 important role in cancer [34]. IGF2 signals through type-1 insulin-like growth factor receptor
371 (IGF1R), which is one of the crucial receptor tyrosine kinases implicated in the development
372 of gastroenteropancreatic neuroendocrine neoplasms [35]. Currently, the available agents
373 targeting IGF2 signaling include small-molecule tyrosine kinase inhibitor against IGF1R (e.g.
374 linsitinib), monoclonal antibodies against IGF1R (e.g. ganitumab, dalotuzumab, figitumumab,
375 cixutumumab), and blocking antibodies against IGF (MEDI-573 and BI 836845) [36].
376 Several multi-center single or combinational Phase I/II studies of these agents are still
377 ongoing and more favorable outcomes are expected to be revealed in the near future.
378 Ganitumab, a fully human antibody against IGF1R, for example, is well tolerated and has
379 antitumor activity in patients with metastatic Ewing family tumors or desmoplastic small
380 round cell tumors [37]. Cixutumumab, another fully human monoclonal antibody targeting
381 IGF1R, which we found to have significant suppressive effects on human ESCC tumor

xenografts in nude mice [12], was reported to be well-tolerated and active in relapsed thymoma in a phase II trial [38]. The results of our present study corroborates that treatment with IGF2-neutralizing antibody can inhibit the abilities of CD133-positive ESCC cells to initiate tumor, self-renew, and resist chemotherapeutic drugs **(Figure 2 and Figure 4)**. Likewise, PI3K/AKT inhibitors previously shown to inhibit chemoresistance and metastasis of ESCC [20, 21] were found to be effective in suppressing stemness of CD133-positive CSCs. MicroRNAs can function as negative regulators of target genes by inducing translational repression and mRNA degradation. They are increasingly recognized as useful predictive biomarkers and therapeutic targets for cancer [39]. In this study, we showed that miR-377 mediates the effects of IGF2 on CD133 expression and CSC properties (**Figure 3**).

In conclusion, our new findings not only provide mechanistic insight into the regulatory functions of the IGF2-PI3K/AKT-miR-377-CD133 signaling pathway in tumor initiation, but also rationalize the clinical application of PI3K/AKT inhibitors and IGF2 antibody therapy in targeting tumor-initiating cells and treating human cancer.

5. Acknowledgement

This study was supported by the Research Grants Council of the Hong Kong SAR (GRF project no. HKU762610M, 17103814), National Natural Science Foundation of China (81672953, 81472790), Guangzhou Science and Technology Project (201707010260), Guangdong Natural Science Research Grant (2016A030313838), the University of Hong Kong Seed Funding Programme for Basic Research (Project no. 201211159003) and Small Project Funding (project no. 201409176113). We thank Professor Simon Law, Dr Nikki PY Lee and Dr. Kin Tak Chan (Department of Surgery, University of Hong Kong); and Professor XY Guan (Department of Clinical Oncology, University of Hong Kong) for their help in providing clinical samples. We thank Professor Yutaka Shimada (University of Toyama, Toyama, Japan) and DSMZ for the KYSE270 cell line, and Dr. Hitoshi Kawamata (Dokkyo University School of Medicine, Tochigi, Japan) for the T.Tn cell line. Flow cytometry and cell sorting were performed and analyzed in the University of Hong Kong Li Ka Shing Faculty of Medicine Faculty Core Facility.

6. References

[1] Y. Zhang, Epidemiology of esophageal cancer, World J. Gastroenterol., 19 (2013) 5598-5606.

[2] N.A. Dallas, L. Xia, F. Fan, M.J. Gray, P. Gaur, G. van Buren, 2nd, S. Samuel, M.P. Kim, S.J. Lim, L.M. Ellis, Chemoresistant colorectal cancer cells, the cancer stem cell phenotype, and increased sensitivity to insulin-like growth factor-I receptor inhibition, Cancer Res., 69 (2009) 1951-1957.

[3] T.K. Lee, A. Castilho, V.C. Cheung, K.H. Tang, S. Ma, I.O. Ng, CD24(+) liver tumor-initiating cells drive self-renewal and tumor initiation through STAT3-mediated NANOG regulation, Cell stem cell, 9 (2011) 50-63.

[4] A. Weigmann, D. Corbeil, A. Hellwig, W.B. Huttner, Prominin, a novel microvilli-specific polytopic membrane protein of the apical surface of epithelial cells, is targeted to plasmalemmal protrusions of non-epithelial cells, Proc. Natl. Acad. Sci. U. S. A., 94 (1997) 12425-12430.

[5] S. Ma, K.H. Tang, Y.P. Chan, T.K. Lee, P.S. Kwan, A. Castilho, I. Ng, K. Man, N. Wong, K.F. To, B.J. Zheng, P.B. Lai, C.M. Lo, K.W. Chan, X.Y. Guan, miR-130b Promotes CD133(+) liver tumor-initiating cell growth and self-renewal via tumor protein 53-induced nuclear protein 1, Cell stem cell, 7 (2010) 694-707.

[6] M. Schneider, J. Huber, B. Hadaschik, G.M. Siegers, H.H. Fiebig, J. Schuler, Characterization of colon cancer cells: a functional approach characterizing CD133 as a potential stem cell marker, BMC Cancer, 12 (2012) 96.

[7] A. Fathi, H. Mosaad, S. Hussein, M. Roshdy, E.I. Ismail, Prognostic significance of CD133 and ezrin expression in colorectal carcinoma, IUBMB Life, 69 (2017) 328-340.

[8] Z.X. Qiu, S. Zhao, X.M. Mo, W.M. Li, Overexpression of PROM1 (CD133) confers poor prognosis in non-small cell lung cancer, Int. J. Clin. Exp. Pathol., 8 (2015) 6589-6595.

[9] B. Li, W.W. Xu, L. Han, K.T. Chan, S.W. Tsao, N.P. Lee, S. Law, L.Y. Xu, E.M. Li, K.W. Chan, Y.R. Qin, X.Y. Guan, Q.Y. He, A.L. Cheung, MicroRNA-377 suppresses initiation and progression of esophageal cancer by inhibiting CD133 and VEGF, Oncogene, 36 (2017) 3986-4000.

[10] J. Zha, M.R. Lackner, Targeting the insulin-like growth factor receptor-1R pathway for cancer therapy, Clin. Cancer Res., 16 (2010) 2512-2517.

[11] I. Heidegger, P. Massoner, N. Sampson, H. Klocker, The insulin-like growth factor (IGF) axis as an anticancer target in prostate cancer, Cancer Lett., 367 (2015) 113-121.

[12] B. Li, S.W. Tsao, K.W. Chan, D.L. Ludwig, R. Novosyadlyy, Y.Y. Li, Q.Y. He, A.L. Cheung, Id1-induced IGF-II and its autocrine/endocrine promotion of esophageal cancer progression and chemoresistance--implications for IGF-II and IGF-IR-targeted therapy, Clin. Cancer Res., 20 (2014) 2651-2662.

[13] W.W. Xu, B. Li, X.Y. Guan, S.K. Chung, Y. Wang, Y.L. Yip, S.Y. Law, K.T. Chan, N.P. Lee, K.W. Chan, L.Y. Xu, E.M. Li, S.W. Tsao, Q.Y. He, A.L. Cheung, Cancer cell-secreted IGF2 instigates fibroblasts and bone marrow-derived vascular progenitor cells to promote cancer progression, Nature communications, 8 (2017) 14399.

[14] Y. Shimada, M. Imamura, T. Wagata, N. Yamaguchi, T. Tobe, Characterization of 21 newly established esophageal cancer cell lines, Cancer, 69 (1992) 277-284.

[15] H. Kawamata, T. Furihata, F. Omotehara, T. Sakai, H. Horiuchi, Y. Shinagawa, J. Imura, Y. Ohkura, M. Tachibana, K. Kubota, A. Terano, T. Fujimori, Identification of genes differentially expressed in a newly isolated human metastasizing esophageal cancer cell line, T.Tn-AT1, by cDNA microarray, Cancer Sci., 94 (2003) 699-706.

[16] F. Vazquez, S.R. Grossman, Y. Takahashi, M.V. Rokas, N. Nakamura, W.R. Sellers, Phosphorylation of the PTEN tail acts as an inhibitory switch by preventing its recruitment into a protein complex, J. Biol. Chem., 276 (2001) 48627-48630.

[17] F. Liu, S. Wagner, R.B. Campbell, J.A. Nickerson, C.A. Schiffer, A.H. Ross, PTEN enters the nucleus by diffusion, J. Cell. Biochem., 96 (2005) 221-234.

[18] B. Li, W.W. Xu, X.Y. Guan, Y.R. Qin, S. Law, N.P. Lee, K.T. Chan, P.Y. Tam, Y.Y. Li, K.W. Chan, H.F. Yuen, S.W. Tsao, Q.Y. He, A.L. Cheung, Competitive Binding Between Id1 and E2F1 to Cdc20 Regulates E2F1 Degradation and Thymidylate Synthase Expression to Promote Esophageal Cancer Chemoresistance, Clin. Cancer Res., 22 (2016) 1243-1255.

[19] B. Li, P.Y. Cheung, X. Wang, S.W. Tsao, M.T. Ling, Y.C. Wong, A.L. Cheung, Id-1 activation of PI3K/Akt/NFkappaB signaling pathway and its significance in promoting survival of esophageal cancer cells, Carcinogenesis, 28 (2007) 2313-2320.

[20] B. Li, W.W. Xu, A.K.Y. Lam, Y. Wang, H.F. Hu, X.Y. Guan, Y.R. Qin, N. Saremi, S.W. Tsao, Q.Y. He, A.L.M. Cheung, Significance of PI3K/AKT signaling pathway in metastasis of esophageal squamous cell carcinoma and its potential as a target for anti-metastasis therapy, Oncotarget, 8 (2017) 38755-38766.

[21] B. Li, J. Li, W.W. Xu, X.Y. Guan, Y.R. Qin, L.Y. Zhang, S. Law, S.W. Tsao, A.L. Cheung, Suppression of esophageal tumor growth and chemoresistance by directly targeting the PI3K/AKT pathway, Oncotarget, 5 (2014) 11576-11587.

[22] D. Hang, H.C. Dong, T. Ning, B. Dong, D.L. Hou, W.G. Xu, Prognostic value of the stem cell markers CD133 and ABCG2 expression in esophageal squamous cell carcinoma, Dis. Esophagus, 25 (2012) 638-644.

[23] H. Okamoto, F. Fujishima, Y. Nakamura, M. Zuguchi, Y. Ozawa, Y. Takahashi, G. Miyata, T. Kamei, T. Nakano, Y. Taniyama, J. Teshima, M. Watanabe, A. Sato, N.

493 Ohuchi, H. Sasano, Significance of CD133 expression in esophageal squamous cell
494 carcinoma, World J. Surg. Oncol., 11 (2013) 51.
495 [24] V. Barroca, D. Lewandowski, A. Jaracz-Ros, S.N. Hardouin, Paternal Insulin-like
496 Growth Factor 2 (Igf2) Regulates Stem Cell Activity During Adulthood, EBioMedicine,
497 15 (2017) 150-162.
498 [25] H. Yan, P. Bu, Non-coding RNAs in cancer stem cells, Cancer Lett., (2018).
499 [26] H. Lv, G. Lv, Q. Han, W. Yang, H. Wang, Noncoding RNAs in liver cancer stem cells:
500 The big impact of little things, Cancer Lett., 418 (2018) 51-63.
501 [27] N. Garg, D. Bakhshinyan, C. Venugopal, S. Mahendram, D.A. Rosa, T. Vijayakumar, B.
502 Manoranjan, R. Hallett, N. McFarlane, K.H. Delaney, J.M. Kwiecien, C.C. Arpin, P.S.
503 Lai, R.F. Gomez-Biagi, A.M. Ali, E.D. de Araujo, O.A. Ajani, J.A. Hassell, P.T.
504 Gunning, S.K. Singh, CD133+ brain tumor-initiating cells are dependent on STAT3
505 signaling to drive medulloblastoma recurrence, Oncogene, 36 (2017) 606-617.
506 [28] J. Long, C. Jiang, B. Liu, Q. Dai, R. Hua, C. Chen, B. Zhang, H. Li, Maintenance of
507 stemness by miR-589-5p in hepatocellular carcinoma cells promotes chemoresistance
508 via STAT3 signaling, Cancer Lett., (2017).
509 [29] J.W. Jang, Y. Song, S.H. Kim, J.S. Kim, K.M. Kim, E.K. Choi, J. Kim, H.R. Seo,
510 CD133 confers cancer stem-like cell properties by stabilizing EGFR-AKT signaling in
511 hepatocellular carcinoma, Cancer Lett., 389 (2017) 1-10.
512 [30] F. Islam, V. Gopalan, R. Wahab, R.A. Smith, A.K. Lam, Cancer stem cells in
513 oesophageal squamous cell carcinoma: Identification, prognostic and treatment
514 perspectives, Crit. Rev. Oncol. Hematol., 96 (2015) 9-19.
515 [31] F.B. Rassouli, M.M. Matin, M. Saeinasab, Cancer stem cells in human digestive tract
516 malignancies, Tumour Biol., 37 (2016) 7-21.

[32] K.H. Tang, Y.D. Dai, M. Tong, Y.P. Chan, P.S. Kwan, L. Fu, Y.R. Qin, S.W. Tsao, H.L. Lung, M.L. Lung, D.K. Tong, S. Law, K.W. Chan, S. Ma, X.Y. Guan, A CD90(+) tumor-initiating cell population with an aggressive signature and metastatic capacity in esophageal cancer, Cancer Res., 73 (2013) 2322-2332.

[33] C. Chen, F. Luo, Q. Yang, D. Wang, P. Yang, J. Xue, X. Dai, X. Liu, H. Xu, J. Lu, A. Zhang, Q. Liu, NF-kappaB-regulated miR-155, via repression of QKI, contributes to the acquisition of CSC-like phenotype during the neoplastic transformation of hepatic cells induced by arsenite, Mol. Carcinog., 57 (2018) 483-493.

[34] S.M. Kessler, J. Haybaeck, A.K. Kiemer, Insulin-like growth factor 2 - The oncogene and its accomplices, Curr. Pharm. Des., 22 (2016) 5948-5961.

[35] F. Briest, P. Grabowski, PI3K-AKT-mTOR-signaling and beyond: the complex network in gastroenteropancreatic neuroendocrine neoplasms, Theranostics, 4 (2014) 336-365.

[36] W.T. Iams, C.M. Lovly, Molecular pathways: Clinical applications and future direction of insulin-like growth factor-1 receptor pathway blockade, Clin. Cancer Res., 21 (2015) 4270-4277.

[37] W.D. Tap, G. Demetri, P. Barnette, J. Desai, P. Kavan, R. Tozer, P.W. Benedetto, G. Friberg, H. Deng, I. McCaffery, I. Leitch, S. Badola, S. Chang, M. Zhu, A. Tolcher, Phase II study of ganitumab, a fully human anti-type-1 insulin-like growth factor receptor antibody, in patients with metastatic Ewing family tumors or desmoplastic small round cell tumors, J. Clin. Oncol., 30 (2012) 1849-1856.

[38] A. Rajan, C.A. Carter, A. Berman, L. Cao, R.J. Kelly, A. Thomas, S. Khozin, A.L. Chavez, I. Bergagnini, B. Scepura, E. Szabo, M.J. Lee, J.B. Trepel, S.K. Browne, L.B. Rosen, Y. Yu, S.M. Steinberg, H.X. Chen, G.J. Riely, G. Giaccone, Cixutumumab for patients with recurrent or refractory advanced thymic epithelial tumours: a multicentre, open-label, phase 2 trial, Lancet Oncol., 15 (2014) 191-200.

[39] J. Ni, J. Bucci, L. Chang, D. Malouf, P. Graham, Y. Li, Targeting microRNAs in prostate cancer radiotherapy, Theranostics, 7 (2017) 3243-3259.

7. Figure Legends

Figure 1. IGF2 is essential for maintenance of CSC properties in esophageal cancer. (**A**) Comparison of tumorigenicity of KYSE270-shCON and KYSE270-shIGF2#2 cells in nude mice. (**B**) Tumor incidence in nude mice during serial passage of KYSE270-shCON cells (left flank, black arrow) and KYSE270-shIGF2#2 cells (right flank, white arrow) inoculated at a dose of $2x10^4$ cells. Representative photos of mice bearing subcutaneous tumors taken 60 days after subcutaneous inoculation of cancer cells are shown below. (**C**) IGF2 (50 ng/ml) significantly enhanced serial propagation of tumor spheres in esophageal cancer cells, but addition of LY294002 (5 μM) abolished this effect. (**D**) Effect of IGF2-knockdown on the ability of esophageal cancer cells to initiate and form tumor spheres over serial passages. (**E**) Two ESCC cell lines were treated with 50 ng/ml IGF2 in the presence or absence of 5 μM LY294002 for 48 h, and the expression levels of p-AKT, AKT, and CD133 were detected by western blot. (**F**) Knockdown of IGF2 markedly reduced CD133 expression. Bars, SD; *, $P < 0.05$; **, $P < 0.01$ compared with the control cells.

Figure 2. Effects of PI3K/AKT inhibition on the ability of $CD133^+$ ESCC cells to self renew, form tumors, and resist chemotherapeutic drugs. (**A**) Sphere-forming ESCC cells and adherent counterparts were compared for p-AKT and AKT expressions by western blot. (**B, C**) Treatment with wortmannin or LY294002 for 72 h (**B)**, and PTEN-overexpression (**C**) resulted in marked reduction of CD133 expression in ESCC cells. (**D)** $CD133^+$ KYSE270 cells were more sensitive to PI3K inhibitors wortmannin (10 μM) and LY294002 (10 μM) than $CD133^-$ cells. (**E, F)** Treatment with wortmannin (5 μM) or LY294002 (5 μM) significantly suppressed serial sphere formation ability (**E**), and reduced CD133 expression in sorted $CD133^+$ KYSE270 cells (**F**). (**G**) Nude mice bearing tumor xenografts derived from

CD133$^+$ KYSE270 cells were treated with 0.6 mg/kg wortmannin twice a week for 3 weeks (n = 6). (**H**) Comparison of the ability of CD133$^+$ KYSE270 cells to form spheres in the presence of 5-FU (10 μM), DDP (40 μM), wortmannin (2.5 μM), or a combination of wortmannin and 5-FU or DDP. DMSO-treated cells served as control. Bars, SD; *, $P< 0.05$; **, $P < 0.01$; ***, $P < 0.001$.

Figure 3. IGF2 stimulates PI3K/AKT pathway, which reduces miR-377 expression, to upregulate CD133. (**A**) KYSE270 and T.Tn cells were treated with wortmannin (left panel) or transfected with PTEN (right panel), and qRT-PCR was performed to determine the miR-377 expression level relative to that of corresponding controls. (**B**) qRT-PCR analysis of miR-377 expression in the KYSE270 and T.Tn cells treated with IGF2 (50 ng/ml) in the presence or absence of LY294002 (5 μM). (**C**) Effect of IGF2-knockdown on miR-377 expression in KYSE270 and T.Tn cells. (**D**) Analyses of expression levels of miR-377 (left panel), p-AKT, AKT, and CD133 (right panel) in the tumor xenografts of KYSE270-shCON and KYSE270-shIGF2#2 cells (Figure 1A) by qRT-PCR and western blot, respectively. (**E**) Western blot analysis of CD133 expression in the ESCC cells treated with IGF2 (50 ng/ml) with or without miR-377 transfection (50 nM). (**F, G)** The ESCC cells with IGF2-knockdown were transfected with miR-377 inhibitor or the corresponding control (miRNA inhibitor NC), and then compared with the control cells for the abilities to resist 5-FU treatment (**F**) and to form spheres over serial passages (**G**). (**H**) Proposed model illustrating the mechanism of IGF2 in regulating CD133 expression and CSC properties in ESCC. Bars, SD; * $P < 0.05$; **, $P < 0.01$; ***, $P < 0.001$ compared with controls.

Figure 4. Therapeutic efficacy of IGF2-neutralizing antibody in suppressing ESCC tumorigenicity and chemoresistance *in vivo*. (**A**) Comparison of the ability of ESCC cells to form spheres in the presence of different doses of IGF2-neutralizing antibody. Note that neutralizing antibody against IGF2 inhibited propagation of tumor spheres over serial passages. (**B**) Growth curves of subcutaneous KYSE270 tumors in nude mice treated with IGF2-neutralizing antibody. (**C**) Expression level of miR-377 and protein expression levels of p-AKT, AKT, CD133 were determined by qRT-PCR and western blot, respectively. (**D**) Treatment with IGF2-neutralizing antibody significantly enhanced the sensitivity of KYSE270 tumor xenografts to 5-FU in nude mice. Bars, SD; * $P < 0.05$; **, $P < 0.01$; ***, $P < 0.001$ compared with controls.

Figure 5. Clinicopathological significance of IGF2 and CD133 expressions in ESCC. (**A**) Representative images of ESCC with immunohistochemical staining scores of 0 to 3 for IGF2. (**B**) Immunostaining scores for IGF2 expression in 100 cases of tumors and 80 cases of normal tissues. The mean values are represented by the horizontal lines. An example of a primary ESCC with higher immunohistochemical expression of IGF2 compared with matched normal epithelium is included below the graph. (**C**) Representative images of CD133-negative and CD133-positive tumors (upper panel). An example of CD133 staining in paired primary ESCC tissue and non-tumor tissues (lower panel). (**D**) CD133 expression status in 100 cases of ESCC and 80 cases of normal tissues. (**E**) Kaplan-Meier plots were used to compare overall survival of 100 patients with ESCC stratified according to IGF2 expression level (left panel), CD133 expression status (middle panel), and different IGF2 and CD133 expression statuses (right panel).

Figure 6. Relationship between IGF2 levels and expression of other markers. (A) Correlations between IGF2 and CD133, and between IGF2 and miR-377 in 47 pairs of ESCC and normal tissues. (B) Correlation between IGF2 and CD133 in other cancer types based on data available from TCGA database.

Figure 1

A

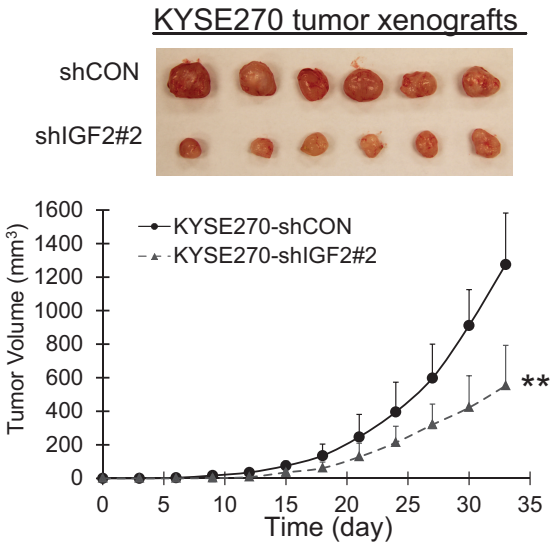

B

KYSE270	Tumor incidence
1st passage:	
shCON	6/6
shIGF2	3/6
2nd passage:	
shCON	6/6
shIGF2	2/6

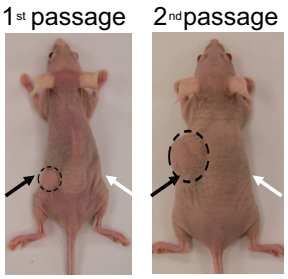

C

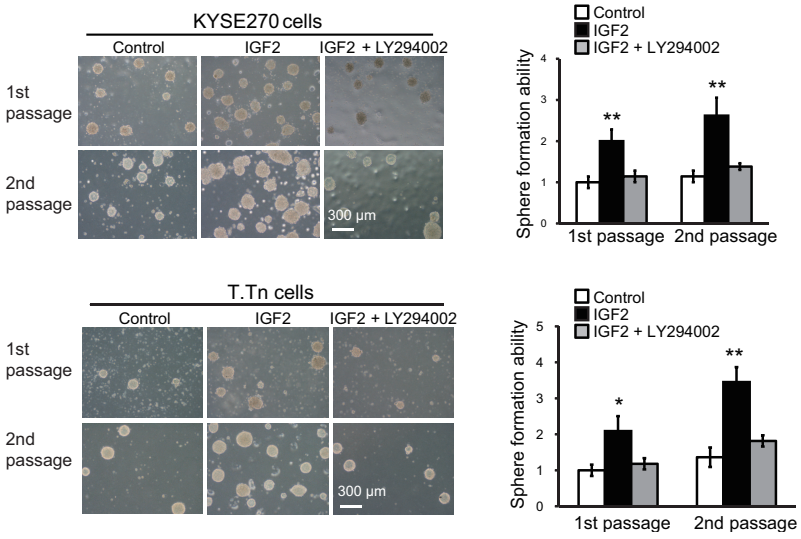

D

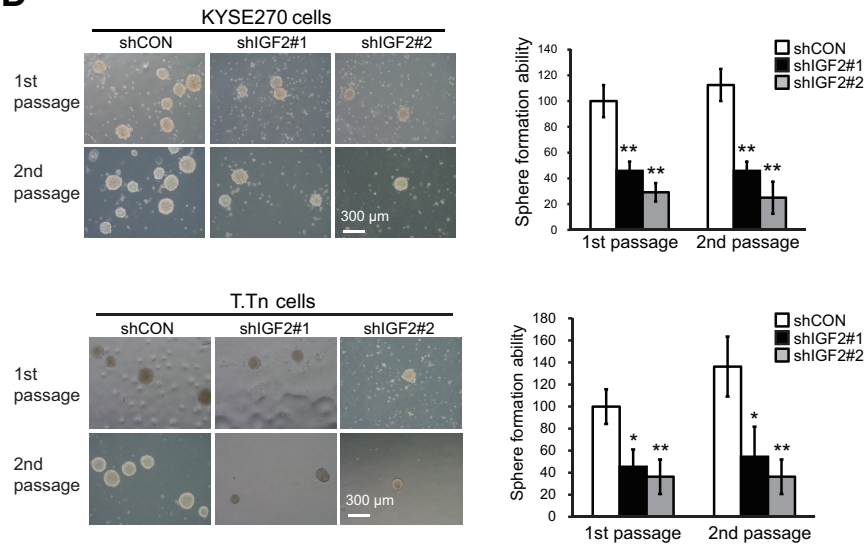

E

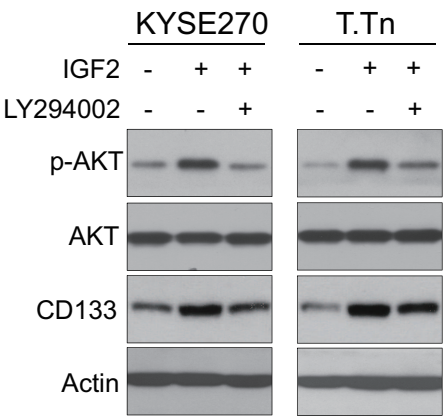

F

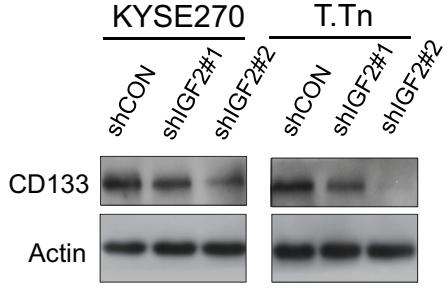

Figure 1

Figure 2

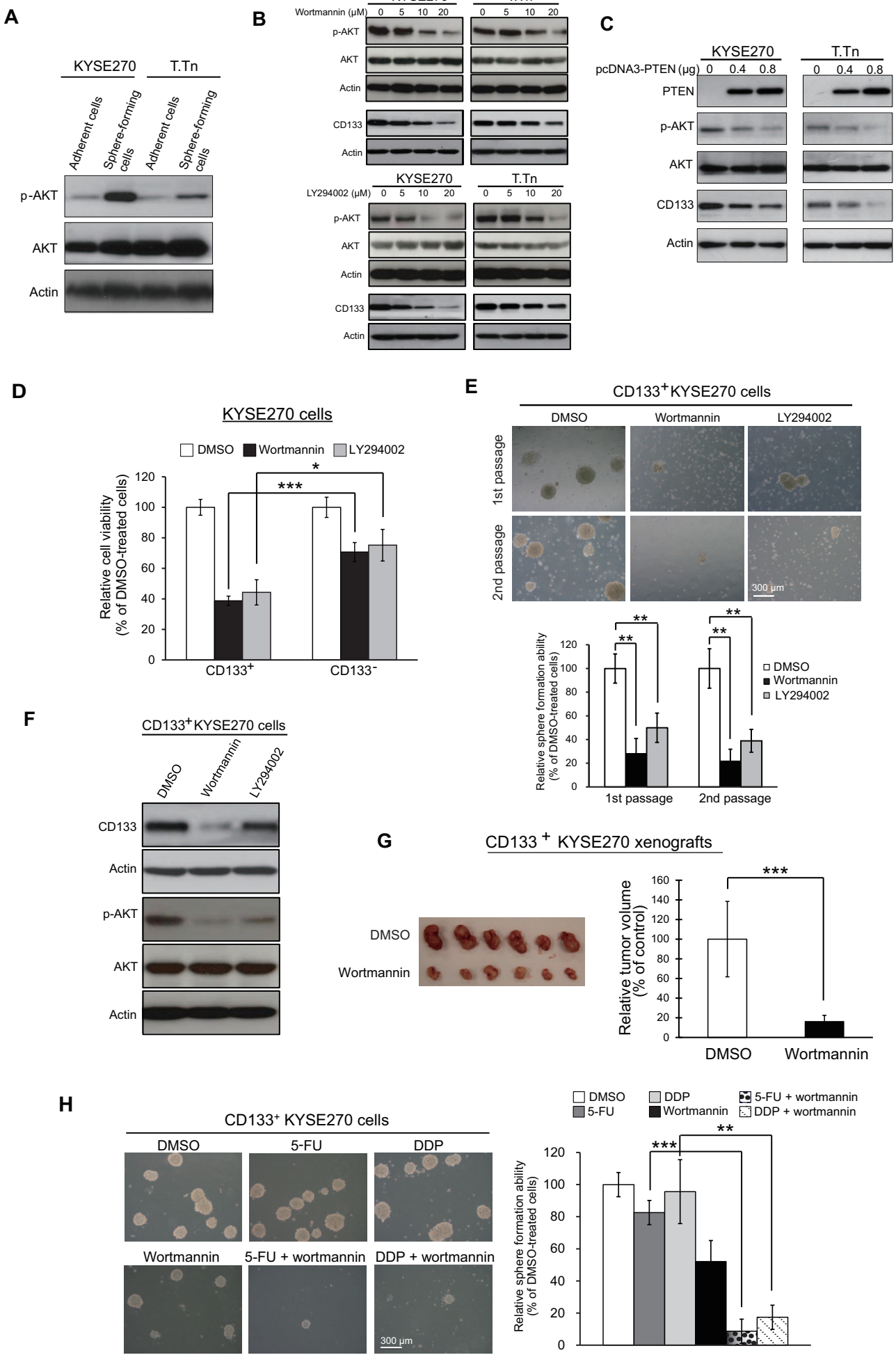

Figure 2

Figure 3

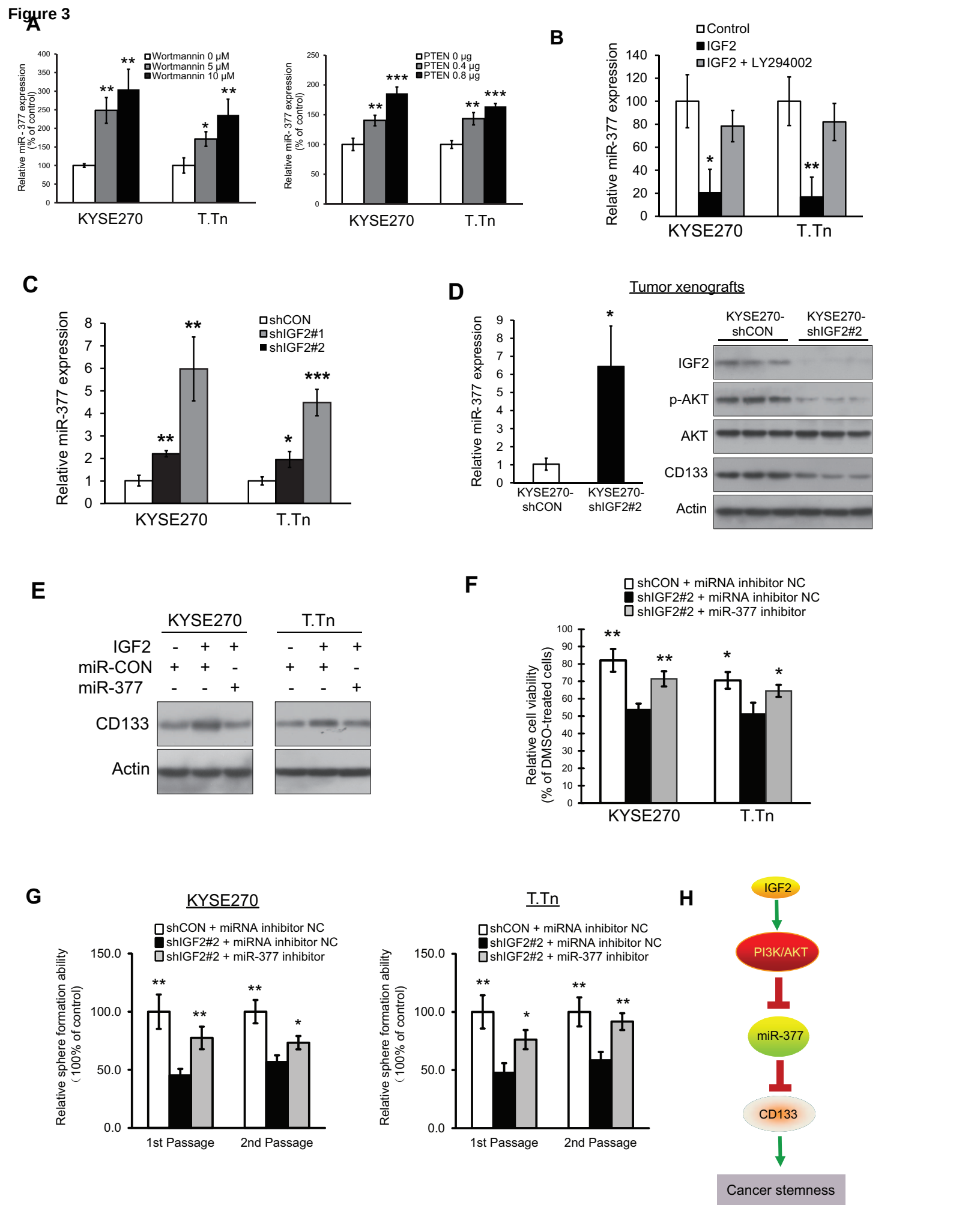

Figure 3

Figure 4

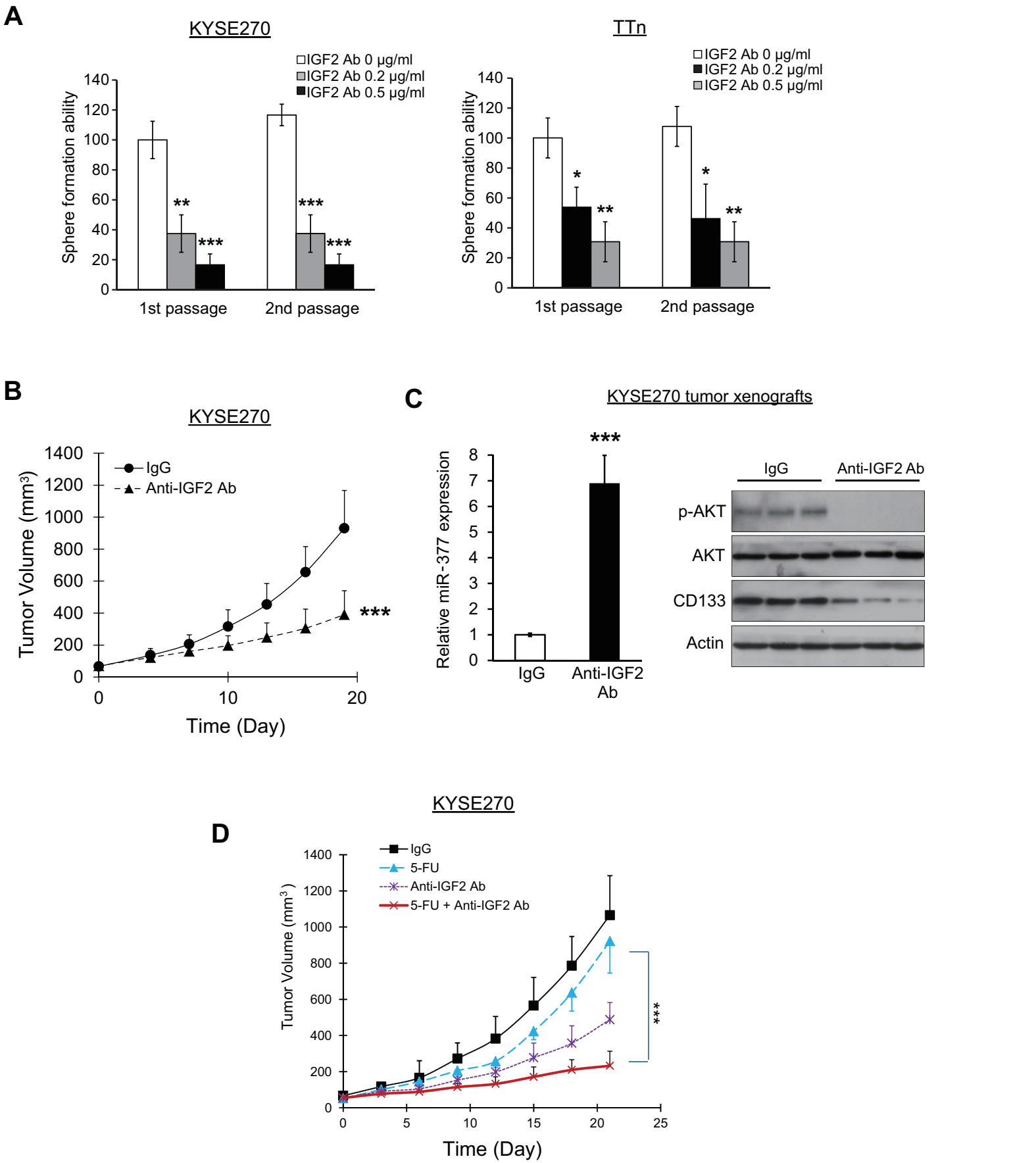

Figure 4

Figure 5

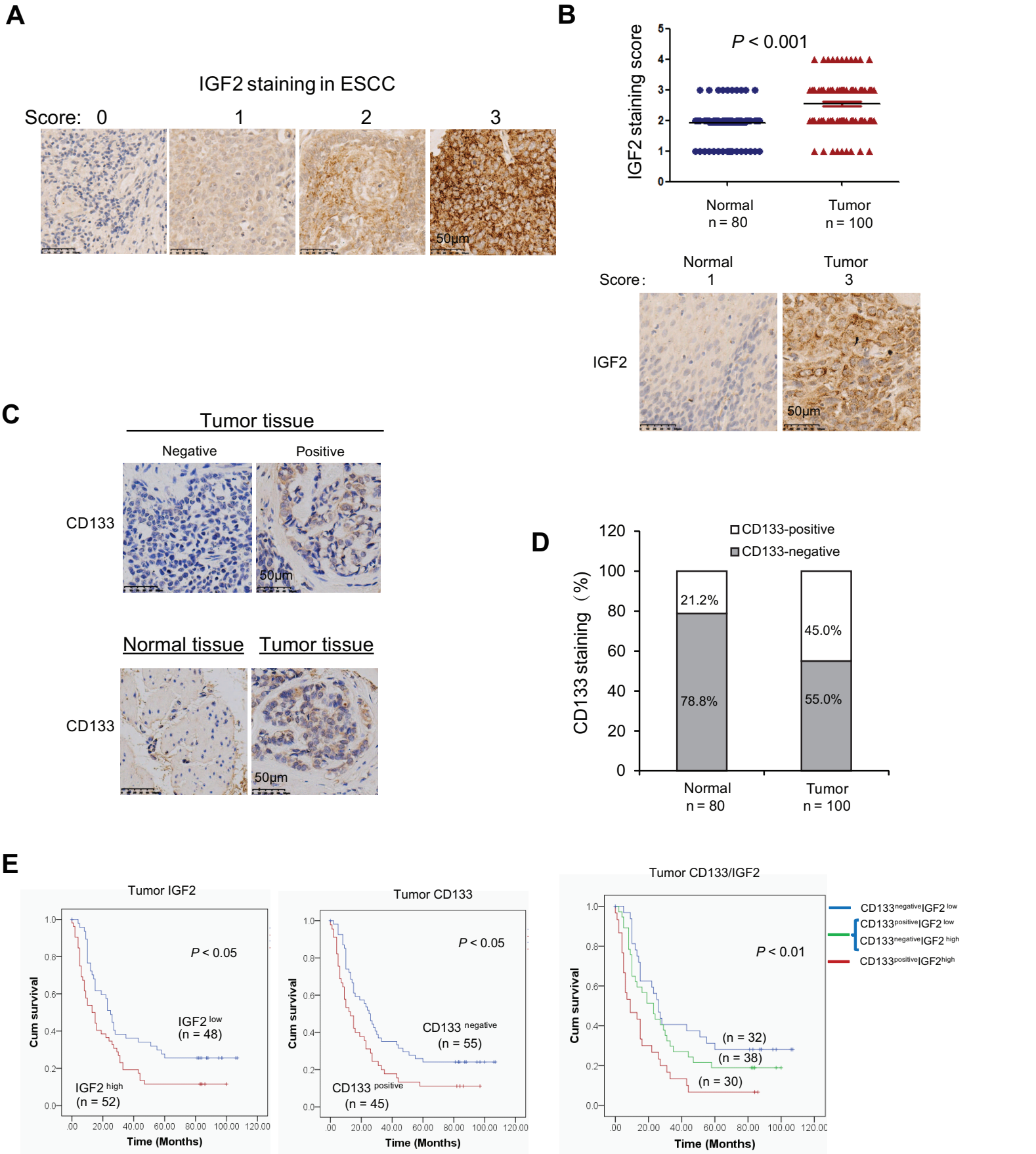

Figure 5

Figure 6

A

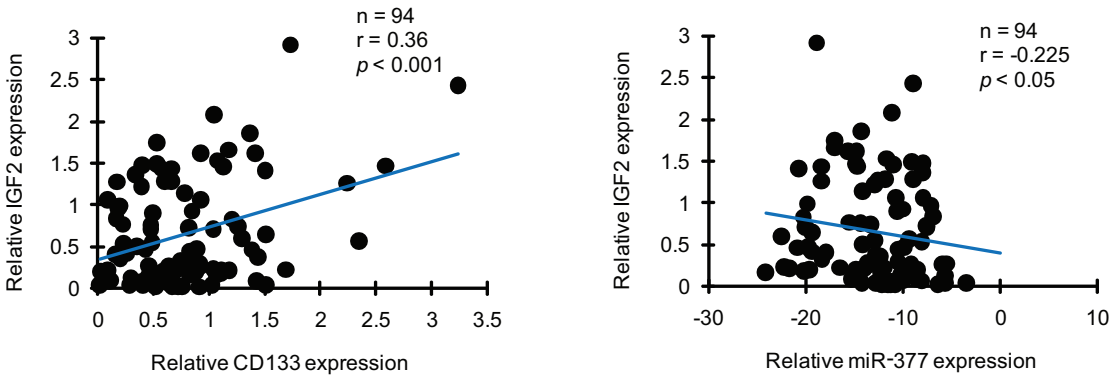

B

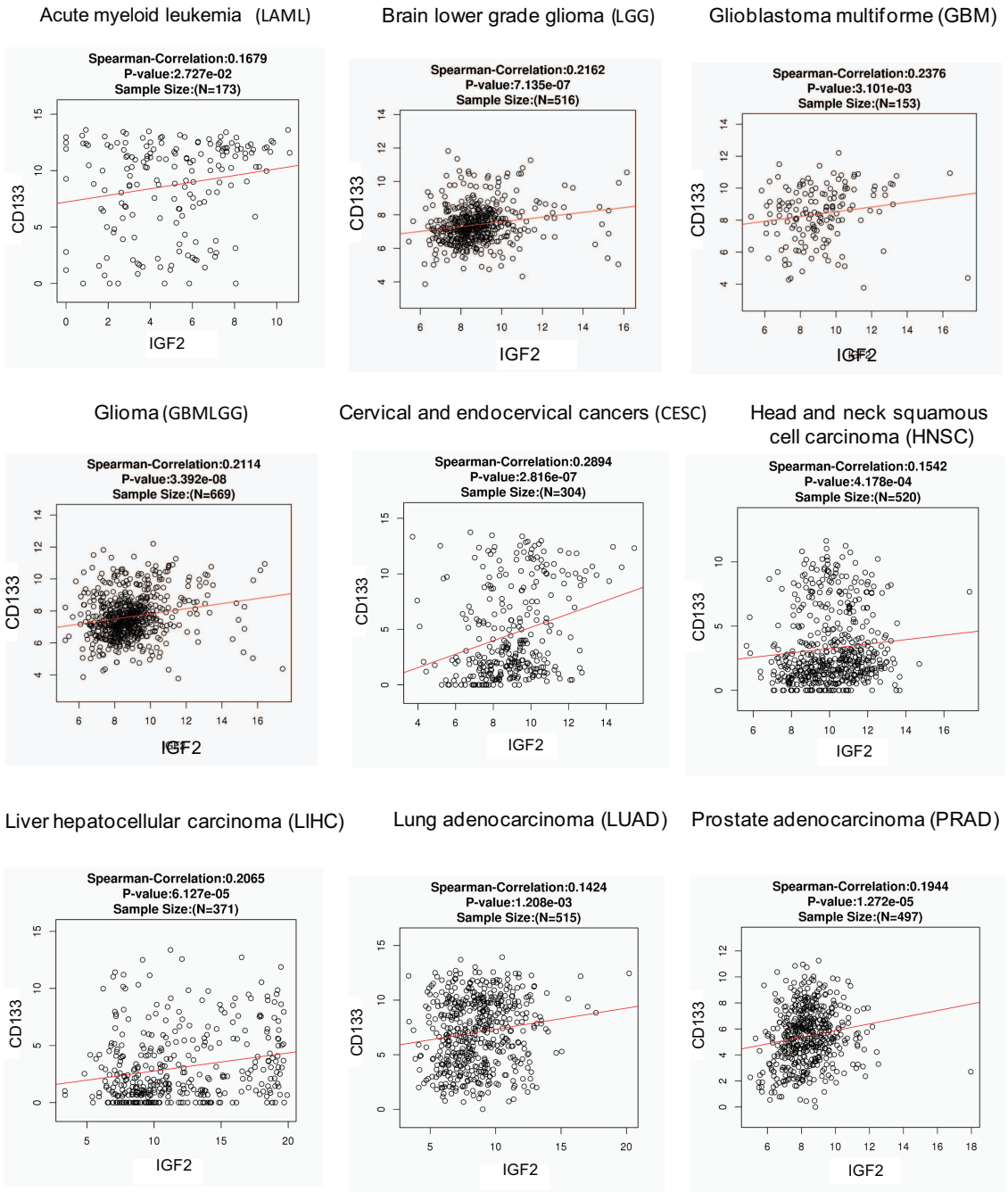

Figure 6

Table 1

Table 1. Correlation between IGF2 expression levels and clinicopathological parameters in 100 cases of ESCC.

Variable	n	Low IGF2	High IGF2	*P* value
Age (years)				
≤55	19	8	11	
>55	81	40	41	0.617
Gender				
Female	26	16	10	
Male	74	32	42	0.117
T-Stage				
1/2	15	11	4	
3/4	82	35	47	**0.047***
N-Stage				
N0	46	27	19	
N1	54	21	33	0.070
M-Stage				
M0	99	48	51	
M1	0	0	0	1.000
Pathologic stage				
Stages I & II	75	34	41	
Stages III & IV	25	14	11	0.367

Table 2

Table 2. Correlation between CD133 expression levels and clinicopathological parameters in 100 cases of ESCC.

Variable	n	Low CD133	High CD133	*P* value
Age (years)				
≤55	19	14	5	
>55	81	41	40	0.078
Gender				
Female	26	14	12	
Male	74	41	33	1.000
T-Stage				
1/2	15	12	3	
3/4	82	40	42	**0.046***
N-Stage				
N0	46	27	19	
N1	54	28	26	0.548
M-Stage				
M0	99	54	45	
M1	0	0	0	1.000
Pathologic stage				
Stages I & II	75	43	32	
Stages III & IV	25	12	13	0.489

Table 3

Table 3. Correlation between CD133/IGF2 expression levels and clinicopathological parameters in 62 cases of ESCC.

Variable	n	$CD133^{low}IGF2^{low}$	$CD133^{high}IGF2^{high}$	*P* value
Age (years)				
≤55	9	6	3	
>55	53	26	27	0.475
Gender				
Female	18	11	7	
Male	44	21	23	0.407
T-Stage				
1/2	8	8	0	
3/4	52	22	30	**0.005****
N-Stage				
N0	26	16	10	
N1	36	16	20	0.208
M-Stage				
M0	60	28	32	
M1	0	0	0	1.000
Pathologic stage				
Stages I & II	45	23	22	
Stages III & IV	17	9	8	1.000

Table 4

Table 4. Cox proportional hazard regression analysis of CD133 and IGF2 expressions for overall survival.

Clinical features	Univariate analysis		Multivariate analysis	
	HR (95% CI)	*P* Value	HR (95% CI)	*P* Value
Age (≤55 years vs >55 years)	1.005 (0.975-1.037)	0.733	-	-
Gender (male vs female)	1.547 (0.807-2.963)	0.189	-	-
T-stage (1/2 vs 3/4)	2.378 (1.006-5.623)	**0.048**	-	-
N-stage (N0 vs N1)	2.243 (1.245-4.040)	**0.007**	1.984 (1.095-3.597)	**0.024**
M-stage (M0 vs M1)	-	-	-	-
Pathological stage (I & II vs III & IV)	1.093 (0.596-2.005)	0.775	-	-
CD133/IGF2 expression ($CD133^{negative}IGF2^{low}$ vs $CD133^{positive}IGF2^{high}$)	2.392 (1.365-4.190)	**0.002**	2.146 (1.217-3.782)	**0.008**

HR, Hazard ratio; CI, Confidence interval
Statistical significance ($P < 0.05$) is shown in bold.

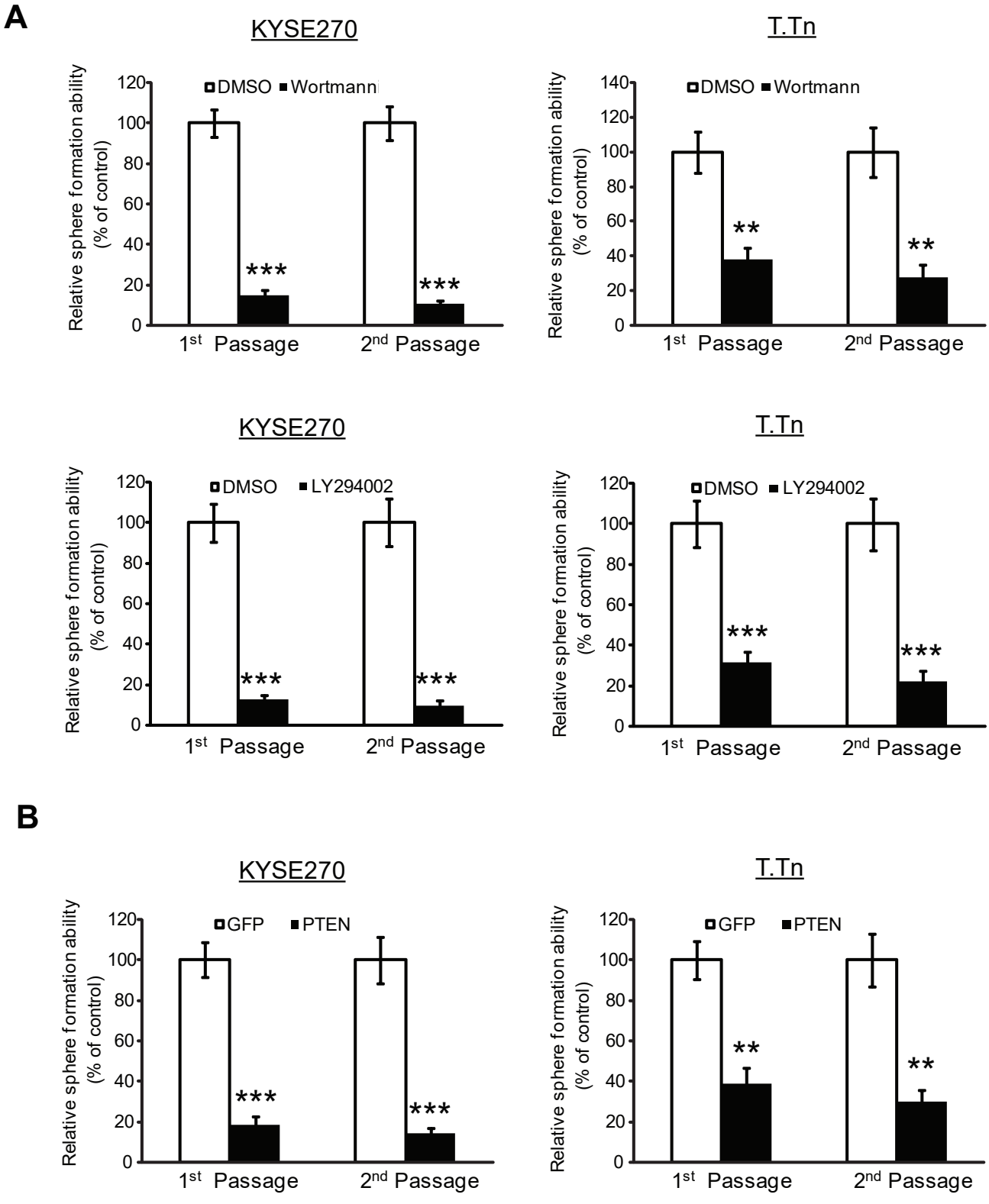

Supplementary Figure 1. Effects of (**A**) PI3K inhibitors and (**B**) PTEN expression on sphere-forming ability of ESCC cells during serial passaging.

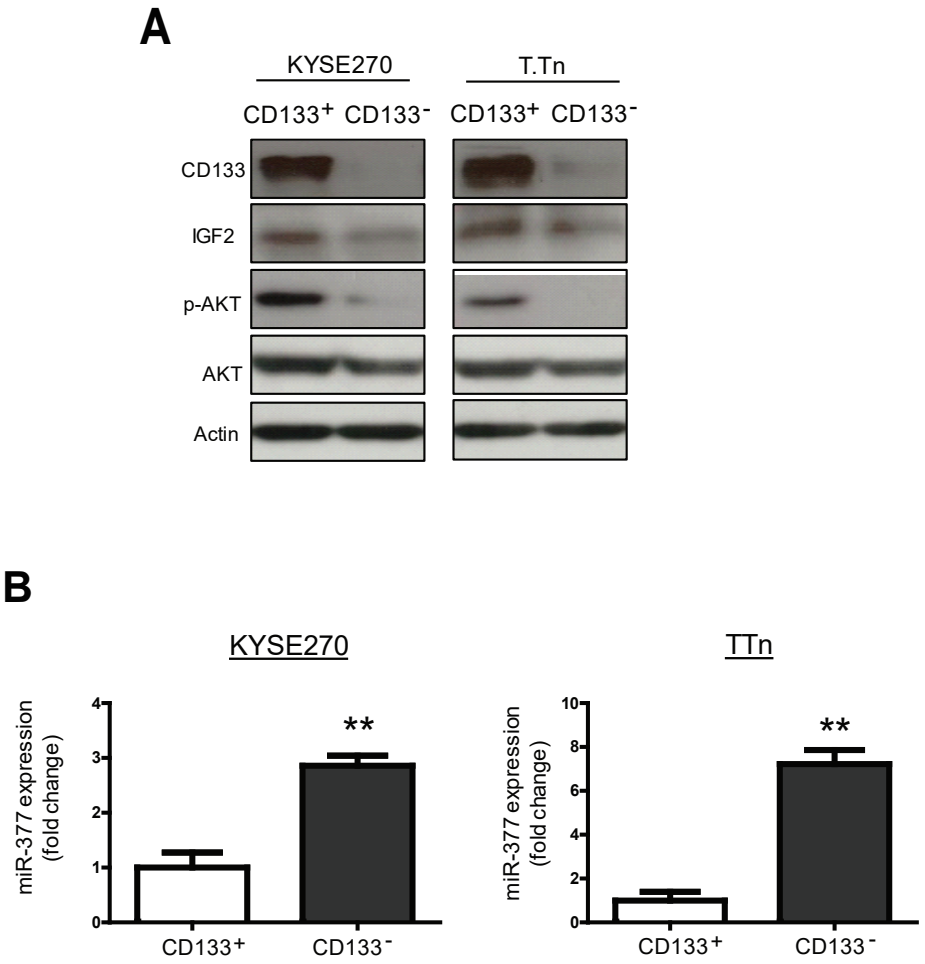

Supplementary Figure 2. **(A)** Western blot showing the expression of CD133, IGF2, p-AKT and AKT in CD133-positive and -negative cells. **(B**） Taqman assay showing the expression of miR-377 in CD133-positive and -negative cells.